# Costimulatory protein 4IgB7H3 drives the malignant phenotype of glioblastoma by mediating immune escape and invasiveness

Lemke, D ; Pfenning, P N ; Sahm, F ; Klein, A C ; Kempf, T ; Warnken, U ; Schnölzer, M ; Tudoran, R ; Weller, M ; Platten, M ; Wick, W

Abstract: PURPOSE: Recent work points out a role of B7H3, a member of the B7-family of costimulatory proteins, in conveying immunosuppression and enforced invasiveness in a variety of tumor entities. Glioblastoma is armed with effective immunosuppressive properties resulting in an impaired recognition and ineffective attack of tumor cells by the immune system. In addition, extensive and diffuse invasion of tumor cells into the surrounding brain tissue limits the efficacy of local therapies. Here, 4IgB7H3 is assessed as diagnostic and therapeutic target for glioblastoma. EXPERIMENTAL DESIGN: To characterize B7H3 in glioblastoma, we conduct analyses not only in glioma cell lines and glioma-initiating cells but also in human glioma tissue specimens. RESULTS: B7H3 expression by tumor and endothelial cells correlates with the grade of malignancy in gliomas and with poor survival. Both soluble 4IgB7H3 in the supernatant of glioma cells and cell-bound 4IgB7H3 are functional and suppress natural killer cell-mediated tumor cell lysis. Gene silencing showed that membrane and soluble 4IgB7H3 convey a proinvasive phenotype in glioma cells and glioma-initiating cells in vitro. These proinvasive and immunosuppressive properties were confirmed in vivo by xenografted 4IgB7H3 gene silenced glioma-initiating cells, which invaded significantly less into the surrounding brain tissue in an orthotopic model and by subcutaneously injected LN-229 cells, which were more susceptible to natural killer cell-mediated cytotoxicity than unsilenced control cells. CONCLUSIONS: Because of its immunosuppressive and proinvasive function, 4IgB7H3 may serve as a therapeutic target in the treatment of glioblastoma.

DOI: https://doi.org/10.1158/1078-0432.CCR-11-0880

# Costimulatory protein 4IgB7H3 drives the malignant phenotype of glioblastoma by mediating immune escape and invasiveness

Dieter Lemke[1,2*], Philipp-Niclas Pfenning[1*], Felix Sahm[3], Ann-Catherine Klein[1], Tore Kempf[4], Uwe Warnken[4], Martina Schnölzer[4], Ruxandra Tudoran[2,5], Michael Weller[6], Michael Platten[2,5], Wolfgang Wick[1,2]

[1]Clinical Cooperation Unit Neurooncology, German Cancer Research Center, Heidelberg, Germany; [2]Department of Neurooncology at the National Center for Tumor Diseases, Heidelberg University Hospital, Germany; [3]Department of Neuropathology, Heidelberg University Hospital, Germany; [4]Protein Analysis Facility, German Cancer Research Center, Heidelberg, Germany; [5]Helmholtz Group for Experimental Neuroimmunology, German Cancer Research Center, Heidelberg, Germany; [6]Department of Neurology, University Hospital Zurich, Switzerland.

* Both authors contributed equally to this work.

**Running title**: 4IgB7H3 in glioblastoma

**Key Words:** Glioblastoma, 4IgB7H3, CD276, Immunosuppression, Invasion

**Address correspondence and reprint requests to**

Wolfgang Wick, M.D.
Department of Neurooncology
University Hospital Heidelberg
Im Neuenheimer Feld 400
D-69120 Heidelberg / Germany
Tel.: +49-6221-567075
Fax: +49-6221-567554
E-mail: wolfgang.wick@med.uni-heidelberg.de

## Statement of translational relevance

Characteristic features of malignant gliomas are their immunosuppressive phenotype and infiltrative growth. Factors like transforming growth factor beta (TGF-β)are relevant in both processes. Here, we show that this is likewise the case for 4IgB7H3, a novel member of the B7-family of costimulatory proteins. We demonstrate B7H3 expression *in vivo* by glioblastoma and endothelial cells and show a correlation with the grade of malignancy and an association with worse clinical outcome. As opposed to other tumors and dendritic cells, 4IgB7H3 is functional in immune and invasion paradigms both cell surface-bound and in a soluble form of 93 kDa. The soluble form is demonstrated to lack the intracellular and the transmembrane domain and was identified in the supernatant of long-term and primary glioma cells. In summary, 4IgB7H3 is an interesting candidate for diagnostic and therapeutic purposes and pivotal for the glioma immune escape as well as gliomas cell invasiveness.

## Abstract

*Purpose*

Recent work points out a role of B7H3, a member of the B7-family of costimulatory proteins, in conveying immunosuppression and enforced invasiveness in a variety of tumor entities. Glioblastoma is armed with effective immunosuppressive properties resulting in an impaired recognition and ineffective attack of tumor cells by the immune system. In addition, extensive and diffuse invasion of tumor cells into the surrounding brain tissue limits the efficacy of local therapies. Here, 4IgB7H3 is assessed as diagnostic and therapeutic target for glioblastoma.

*Experimental Design*

In order to characterize B7H3 in glioblastoma we perform analyses not only in glioma cell lines and glioma initiating cells, but also in human glioma tissue specimens.

*Results*

B7H3 expression by tumor and endothelial cells correlates with the grade of malignancy in gliomas and with poor survival. Both, soluble 4IgB7H3 in the supernatant of glioma cells as

well as cell-bound 4IgB7H3 are functional and suppress natural killer cell-mediated tumor cell lysis. Gene silencing showed that membrane and soluble 4IgB7H3 convey a proinvasive phenotype in glioma cells and glioma initiating cells *in vitro*. These proinvasive and immunosuppressive properties were confirmed *in vivo* by xenografted 4IgB7H3 gene silenced glioma initiating cells, which invaded significantly less into the surrounding brain tissue in an orthotopic model and by subcutaneous injected LN-229 cells, which were more susceptible to NK-cell mediated cytotoxicity compared with unsilenced control cells.

*Conclusions*

Because of its immunosuppressive and proinvasive function, 4IgB7H3 may serve as a therapeutic target in the treatment of glioblastoma.

## Introduction

One of the key biological features of glioblastoma is its ability to suppress the immune system resulting in an impaired recognition and attack of the tumor cells by the immune system. A number of factors have been identified within the last two decades that are held responsible for the immunosuppressive nature of glioblastomas [1-8]. Transforming growth factor-β (TGF-β) turned out to induce apoptosis in T-cells, to downregulate costimulatory proteins on cytotoxic T-cells, natural killer (NK) cells and glioma cells as well as to upregulate immunosuppressive ligands on glioblastoma cells. In addition to the immunosuppressive properties, invasion of tumor cells into the surrounding brain tissue is another hallmark of human glioblastoma. This invasive behaviour limits the feasibility of local treatment like surgical tumor resection or involved-field radiotherapy. Glioblastoma cells usually invade as single cells migrating along white matter tracts implicating the involvement of integrin-mediated signalling pathways and the degradation of components of the extracellular matrix by matrix metalloproteinases (MMP). Recently, two isoforms of a novel member of the B7-family of costimulatory proteins, 2IgB7H3 and 4IgB7H3, have been identified [9, 10]. The latter was more widely expressed in human maturating dendritic cells (DC), T-cells and many human tumor cell lines including glioblastoma [11]. 4IgB7H3 was initially supposed to convey

T-cell activation and to induce IFN-γ production, but more recent evidence suggests that 4IgB7H3 expressed by different human malignancies suppresses NK cells and cytotoxic T-cells. In this regard, NK-mediated lysis of neuroblastoma cell lines was enhanced by 4IgB7H3 neutralizing antibodies [12]. High expression of 4IgB7H3 is associated with a poor prognosis in different tumor entities [13-17]. Apart from the expression on tumor cells, 4IgB7H3 is also specifically upregulated on tumor endothelia [18].

The ligand for B7H3 has not been identified yet. It was postulated that the ligand is expressed on activated T-cells [9]. Hashiguchi et al. [19] delineated Triggering receptor expressed on myeloid cell-like transcript 2 (TLT-2) to be this receptor, but the interaction of B7H3 and TLT-2 resulted in T-cell activation, which could not explain its immunosuppressive action. Moreover, the physical interaction of B7H3 and TLT-2 was not confirmed [20]. Lastly, a soluble form of B7H3 was described to be expressed by human immune cells and by a variety of different tumor cells. This soluble form is cleaved by MMP from the cell surface and is detected in increased levels in the serum of patients with non-small cell lung carcinoma compared with healthy controls and correlated with the tumor burden [21-23].

Factors like TGF-β are relevant in both processes, immunosuppression and invasiveness. Here, we demonstrate that this is likewise the case for 4IgB7H3. We show B7H3 expression *in vivo* by glioblastoma and endothelial cells. 4IgB7H3 was until date only detected in the glioblastoma cell lines U251, A172 and U87 [10]. Furthermore expression of B7H3 in human glioma correlates with the grade of malignancy of astrocytic tumors, ranging from WHO grade II to IV. Importantly, 4IgB7H3 is functional by suppressing NK cell-mediated tumor lysis *in vitro* and *in vivo*. Moreover, glioblastoma-derived soluble 4IgB7H3 suppresses NK cell-lysis. So far, the soluble form in monocytes, DC and activated T-cells was published to be 16.5 kDa [24]. This fragment differs from the 93 kDa fragment detected in the supernatant of glioma initiating cell cultures and glioma cell lines with commercial antibodies. This 93 kDa fragment was not cleaved by MMP from the surface of glioblastoma cells, but by serum endopeptidases. Finally, high B7H3 expression correlates with a lower invasion of CD8

positive cells in human glioblastoma tissue compared with low B7H3 expressing glioblastomas and 4IgB7H3 exerts a proinvasive effect on glioblastoma cells *in vitro* and more important *in vivo*.

## Material and Methods

### *Cells and cell culture*

LN-229 glioma cells were kindly provided by Dr. N. de Tribolet (Lausanne, Switzerland). The cell line was maintained in Dulbecco's modified Eagle's medium containing 10% fetal calf serum and penicillin (100 IU/mL)/streptomycin (100 lg/mL) [25]. For the generation of glioma-initiating cell (GIC) cultures, tumor samples were obtained from adult patients diagnosed with glioblastoma after informed consent. The tumor and the GIC culture methods were modified from Svendsen et al. [26] as previously described [27]. Glioma characteristic chromosomal abnormalities have been verified by array comparative genome hybridization (B. Radlwimmer, Department of Molecular genetics, German Cancer Research Center Heidelberg). Lentiviral knock-down of 4IgB7H3 and control knock-down cells were produced with lentiviral sh 4IgB7H3 and control particles from Santa Cruz Biotechnology (Santa Cruz, CA, USA; Cat. no.: sc-45444-V and sc-108080). The unselected 4IgB7H3 knock-down cells were named sh 4IgB7H3 pool cells. From these cells a clonal knock-down was selected with a higher knock-down rate, which was termed sh 4IgB7H3 clone19. Human Cerebral Microvascular Endothelial Cells (HCMEC) and Human Brain Vascular Pericytes were purchased from Sciencell (Carlsbad, CA, USA).

Lysates for immunoblots and cell culture supernatants were prepared as described previously [28, 29]. Briefly, supernatants were generated for 72 h after plating $3x10^6$ cells in serum-free medium. Serum-free supernatants were concentrated with the Centriplus centrifugal filter device YM-3 (3000-Da cut-off; Millipore, Schwalbach, Germany). Afterwards, a Bradford assay was performed to assure that equal amounts of supernatant-derived

protein were used for the NK cell lysis assays or immunoblot analysis. To unravel the mechanisms how 4IgB7H3 is cleaved by glioblastoma cells and how 4IgB7H3 is regulated $1.25x10^6$ LN-229 cells were seeded in serum-free medium and the following compounds and treatments were used:

1. To evaluate hypoxia cells were incubated for 48 h in serum-free medium under hypoxic conditions at 1 % $O_2$ and compared with cells that were kept at 21 % $O_2$.
2. To evaluate the influence of PKC activation, cells were incubated with phorbol 12-myristate 13-acetate (PMA) (Sigma-Aldrich, Taufkirchen, Germany) diluted in DMSO at a final concentration of 100 nM for 48 h [30].
3. The influence of TGF-β inhibition was tested with LY 2157299, a TGF-β receptor kinase I inhibitor at 25 nM (Axon Medchem BV, Groningen, The Netherlands) (30) or the synthetic furin inhibitor, decanoyl-Arg-Val-Lys-Arg-chloromethylketone (dec-RVKR-cmk) (Bachem, Heidel-berg, Germany), which was diluted in methanol. Cells were incubated at 15 µM. New furin inhibitor was added every 12 h [31].
4. To examine whether 4IgB7H3 is cleaved by MMP, the MMP inhibitor ilomastat [22] was used at concentrations of 5-10 µM (Chemicon International, Temecula, CA). Respective DMSO controls were included.

Afterwards, cells were collected to perform qRT-PCR, immunoblots of supernatants and lysates and flow cytometry analysis. All compounds used were shown to be functional in other assays.

***Immunoblot analysis***

Cells were lysed in 50 mM Tris–HCl (pH 8) containing 120 mM NaCl, 5 mM EDTA, 0.5% Nonidet P-40, 2 µg/ml aprotinin, 10 µg/ml leupeptin (Sigma-Aldrich), and 100 µg/ml phenylmethylsulfonyl fluoride (PMSF). Protein levels were analyzed by immunoblot using 30 µg of protein per lane with the respective antibodies in the concentrations recommended by the manufacturer [29]. The antibodies used were goat polyclonal anti-human B7H3 (R&D, Minneapolis, MN, USA) and rabbit anti-human anti-B7H3 antibody HPA 017139 (Atlas

Antibodies, Stockholm, Sweden). Protein bands were visualized using horseradish peroxidase-coupled secondary antibodies (Sigma-Aldrich). Equal protein loading was ascertained by Ponceau S staining as well as alpha-tubulin stainings with mouse anti-$\alpha$-tubulin antibody (Sigma Aldrich) and rabbit anti $\beta$-actin antibody (Cell Signalling, Danvers, MA, USA).

***Exosome isolation***

Serum free conditioned medium from human glioblastoma cells was collected after 48 h. Microvesicles were purified by differential centrifugation steps (300g/10min; 2000g/20min and 10,000g/30min), pelleted by ultracentrifugation at 175,000g for 60min and washed in PBS. Exosomes were identified by immunoblotting using the exosomal marker protein CD9 (mouse anti-human CD9; 1:1000; Chemicon Temecula, CA).

***Flow cytometry***

For flow cytometry, cells were dissociated with accutase, washed and stained with goat polyclonal anti-human B7H3 1:100 (R&D) or respective isotype control. As secondary antibody donkey Alexa 488 anti-goat antibody was used (Invitrogen, Karlsruhe, Germany) and fluorescence in a total of 10,000 events per condition was detected. Cells were analyzed with a BD-FACS Canto II flow cytometer (BD Biosciences, Heidelberg, Germany), final data were processed with the help of FlowJo flow cytometry analysis software (Tree Star, Ashland, OR, USA). Specific fluorescence intensity (SFI) was calculated by using the mean fluorescence signal of B7H3 divided by the mean fluorescence isotype signal.

***Quantitative Real-Time PCR (qRT-PCR)***

Total RNA was extracted using a RNA purification system (Qiagen, Hilden, Germany) and treated with RNase-free DNase I to remove genomic DNA (Roche, Mannheim, Germany). cDNA was prepared from 5 lg of total RNA using Superscript RNase H–Reverse Transcriptase (Invitrogen, Karlsruhe, Germany) and random hexamers (Sigma-Aldrich,

Taufkirchen, Germany). For qRT-PCR, gene expression was measured in an ABI Prism 7000 Sequence Detection System (Applied Biosystems, Foster City, CA, USA) with SYBR Green Master Mix (Eurogentec, Cologne, Germany) and primers at optimized concentrations [32]. Primers (Sigma-Aldrich) were selected to span exon–exon junctions. The sequence for human 4IgB7H3 and the housekeeping gene glyceraldehyde-3-phosphate dehydrogenase (GAPDH) were as follows: 4IgB7H3 forward primer 5'- CATCACACCCCAGAGAAGCC -3', reverse primer 5'- AGAGGGCCGTG CGGTTGGCA -3', GAPDH primers have been described [33]. Standard curves were generated for each gene and the amplification was 90–100% efficient. Relative quantification of gene expression was determined by comparison of threshold values. All results were normalized to GAPDH.

***Mass spectrometry analysis***

*Probe preparation*: The band corresponding to 4IgB7H3-immunostained areas on the immunoblot were excised from SDS-PAGE. Gel pieces were consecutively washed with water and 50% acetonitrile, reduced with 10 mM DTT at 56°C for 1 h and alkylated with 55 mM iodoacetamide (Sigma Aldrich) at 25°C for 30 min in the dark. After alkylation, gel plugs were repeatedly washed with water and 50% acetonitrile, dehydrated with 100% acetonitrile and air-dried. The dried gel plugs were reswollen in 40 mM ammonium bicarbonate containing 17 ng/µl sequencing grade modified trypsin (Promega, Mannheim, Germany). Following enzymatic digestion overnight at 37°C, peptides were repeatedly extracted with 0.1% TFA and acetonitrile/0.1% TFA 50:50 (v/v). The combined solutions were dried in a speed-vac for 2 h at 37°C. Peptides were redissolved in 5 µl 0.1% TFA by sonication for 10 min and applied for ESI-MS/MS analysis.

*Orbitrap Mass spectrometry analysis:* NanoLC-MS/MS analysis was performed using the nanoACQUITY (Waters, Eschborn, Germany) coupled to a nanoESI- LTQ-Orbitrap mass spectrometer (Thermo Scientific, Bremen, Germany) using a stepped linear acetonitrile/water gradient ranging from 5% to 90% within 45 min. For enhancing the number of detected peptides, a targeted proteomics approach was performed for the identification of 4IgB7H3

(gi67188443, CD276 antigen isoform a, Homo sapiens). Only peptide masses obtained from an in silico trypsin digestion of 4IgB7H3 using a MS-Digest tool from the online ProteinProspector v5.7.2 software (UCSF, San Francisco, USA) were isolated and fragmented by the Orbitrap. Processed data were searched against the NCBInr database using the Mascot algorithm version v2.2.0 (Matrix Science Ltd., London, UK). The taxonomy homo sapiens was selected for Mascot searches.

***NK lysis assay***

Peripheral blood lymphocytes (PBL) were isolated from whole blood samples of healthy donors by Ficoll-Hypaque density gradient centrifugation. NK cells were then isolated from PBL by depletion of non-NK cells using a NK cell isolation kit (Miltenyi Biotec, Bergisch Gladbach, Germany). Isolated $CD56^+/CD3^-$ NK cells were maintained in Roswell Park Memorial Institute (RPMI) 1640 medium (PAA Laboratories, Pasching, Austria) containing 10% fetal bovine serum (FBS; Perbio, Bonn, Germany) and 1000 U/ml interleukin-2 (Immunotools, Friesoythe, Germany) for 5 days at 37°C / 5%$CO_2$.

NK cell cytotoxicity was assessed using $^{51}$chromium ($^{51}$Cr)-release assay [34]. Briefly, labelled glioma cells ($5x10^3$/well) were seeded in triplicates into a U-shaped 96-well microtiter plate and incubated in triplicates with NK effector cells with effective target-to-effector ratios of 1:30, 1:10 and 1:3. Minimum and maximum $^{51}$Cr release was determined by using target cells incubated in medium alone or 10% Triton-X-100 (Applichem, Darmstadt, Germany). After incubation at 37°C/5% $CO_2$ for 4 h, supernatants were collected from each well and counted in a gamma counter (Packard, Meriden, CT, USA). Specific NK lysis in percent was calculated as follows: [Experimental $^{51}$Cr Release - Minimum Release] / [Maximum Release-Minimum Release] x100.

***Matrigel invasion assay***

The invasive properties of glioma cells were assessed in Boyden chamber assays (BD Biosciences), where a porous membrane (8 µm pore size) coated with matrigel matrix

separates upper and lower wells. Glioma cells were harvested in enzyme-free cell dissociation buffer (Gibco Life Technologies, Karlsruhe, Germany) and a total of $4x10^4$ cells in culture medium were added in triplicates to the upper chamber [35]. NIH 3T3-conditioned medium (0.5 ml) was used as a chemoattractant in the bottom well. Cell invasion was evaluated by counting the number of cells that had migrated across the membrane in five independent fields and expressed as percentage of invasiveness relative to control.

***Spheroid invasion assay***

One x $10^6$ GIC were seeded in neural sphere cell medium (NSCM; Invitrogen, Karlsruhe, Germany) and kept in culture until spheroids had formed. Extracellular matrix gel was prepared as described previously [29]. Glioma cell spheroids were seeded into the collagen gel solution in a 24-well plate in triplicates. After gelation, the gel was covered with medium and cultured at 37°C/5% $CO_2$. Microscopic photographs of the area covered by each spheroid were taken at 0, 24, 48 and 72 h after implantation. For quantification, the mean area which was covered by invaded glioma cells at an indicated time point was measured in intervals of 24 h and compared with the area at 0 h.

***Animal experiments***

Animal work was approved by the governmental authorities (Regierungspräsidium Karlsruhe, Germany) and supervised by institutional animal protection officials in accordance with the National Institutes of Health guidelines *Guide for the Care and Use of Laboratory Animals.*

*Orthotopic brain tumor model*

A total of $1x10^5$ human T269 4IgB7H3 knockdown or T269 control cells were stereotactically implanted into the right striatum of five 6-12-week-old athymic mice (CD1 *nu/nu*; Charles River Laboratories, Wilmington, MA, USA), respectively. Ten weeks after implantation, animals were sacrificed, brains removed and cryosectioned. To access infiltration immunostainings were conducted with rabbit anti-human nestin antibody (Millipore) after

fixation of cryosections with acetone. As secondary antibody, Alexa 488 anti-rabbit antibody (Invitrogen) was used.

*Subcutaneous tumor model:*

Flank injection of human glioma cells and systemic depletion of NK cells were performed as described previously [36]. Briefly, 1 x $10^7$ human LN-229 *B7H3* knockdown cells or LN-229 sh-Ctrl. cells were injected s.c. into the right flank of *CD1 nu/nu* mice after mixing with an equal volume of liquid matrigel (BD Matrigel $^{TM}$ Basement Membrane Mix, BD Biosciences). NK-cell depletion was performed by biweekly i.p. injection of 1,5 µg/ml of rabbit anti-asialo GM1 antibody (Wako Chemicals, Duesseldorf, Germany) starting 2 days before tumor cell injection. Controls were injected with rabbit IgG (Calbiochem, Darmstadt, Germany). Tumor growth was regularly monitored using metric callipers. accordingly. Flow cytometric analysis of spleen cells with rat anti-mouse Dx5 (Ly49B) antibody from Caltag (Burlingame, CA) confirmed NK-cell depletion. After 20 days the mice were sacrificed, tumors were excised, and weighed.

***Immunohistochemistry***

Formalin-fixed paraffin-embedded tissue of human diffuse astrocytomas (WHO grade II, n = 3), anaplastic astrocytomas (WHO grade III, = 7) and glioblastoma (WHO grade IV, n =13) were provided by the Department of Neuropathology, Institute of Pathology, University Hospital Heidelberg, Germany. Sections cut to 3 µm were processed using a Ventana BenchMark XT® immunostainer (Ventana Medical Systems, Tucson, AZ, USA). Staining procedure included a pretreatment with cell conditioner 1 (pH 8) for 60min, followed by incubation with either goat anti-human B7H3 antibody (1:200; R&D, Minneapolis, MN, USA) or mouse anti-human CD8 (1:50; Dako, Glostrup, Denmark) at 37°C for 32 min and, for detection of B7H3, application of rabbit anti-goat immunoglobulins (P0446, DAKO, Glostrup, Denmark) for 32 min at room temperature. Incubation was followed by Ventana standard

signal amplification, UltraWash, counterstaining with one drop of hematoxylin for 4min and one drop of bluing reagent for 4 min. For visualization, ultraView™Universal DAB Detection Kit (Ventana Medical Systems) was used. For quantitative analysis of the B7H3 staining pattern, the immunoreactive score (IRS) was applied. IRS was calculated as product of staining intensity and percentage of positive cells, determined as follows: staining intensity was subdivided into four groups, 0 (negative), 1 (weak), 2 (moderate) and 3 (strong). Percentage of positive cells was regarded as 0 (none), 1 (<10%), 2 (10-50%), 3 (51-80%) and 4 (>80% positive tumor cells). Infiltration of CD8 positive cells was assessed in 4 GBM with high (IRS >8) and 4 GBM with low (IRS <8) B7H3 immunoreactivity. Of each case, four 200x magnification fields were analyzed. Presence of respective cells was scored as either 0 (no positive cells), 1 (single positive cells), 2 (single groups of positive cells), or 3 (several groups of >3 positive cells).

***Fluorescent immunohistochemistry***

The B7H3 colocalization studies on cryosections of human glioblastoma tissue samples were performed after acetone fixation and staining with a goat polyclonal anti-human B7H3 antibody (R&D, Minneapolis, MN, USA), a mouse anti-human CD31 antibody (Dako), a mouse anti-human alpha-smooth muscle actin (SMA) antibody (Sigma Aldrich) and a rabbit anti-human nestin (Millipore). As secondary antibodies, a donkey anti-mouse Cy3 antibody (Dianova, Hamburg, Germany) and an Alexa 750 goat anti-rabbit antibody (Invitrogen) were used. Finally, sections were counterstained with 4,6-diamidino-2-phenylindol (DAPI) and analyzed with a Zeiss Axio Observer Z1 immunofluorescence microscope (Zeiss, Oberkochen, Germany).

***Clinical survival data***

Queries of the Repository of Molecular Brain Neoplasia Data (REMBRANDT, National Cancer Institute, Bethesda, MD) for (CD276) were conducted online in 2011 following the webpage's instructions.

### *Statistical analysis*

Statistical significance was assessed by Student's t-Test (Excel, Microsoft, Seattle, WA, USA). All *in vitro* experiments, reported here were performed at least three times in triplicate or more. For *in vivo* experiments five animals per group were operated. Survival data were plotted by the Kaplan-Meier method and analyzed by the log-rank test.

## Results

### B7H3 is expressed in human glioma tissue specimens and cultured glioma cells

B7H3 is detected in specimens of freshly dissected human glioma tissue by immunohistochemistry and is markedly upregulated in glioma tissue compared with the surrounding brain tissue at the infiltration zone (Fig. 1A). Here, strong B7H3 expression is found in close proximity to blood vessels. The degree of B7H3 expression correlated with the grade of malignancy of different gliomas (Fig. 1A). All of 18 glioblastoma samples tested by immunohistochemistry,(13 samples), and immunofluorescence analysis, (five samples), were positive for B7H3 (Fig. 1A,C and 4D). Queries of the NIH's REMBRANDT brain tumor database, based on Affymetrix gene expression data and survival data, indicated in addition a correlation between decreased survival and increased gene expression of B7H3 in anaplastic astrocytomas (WHO grade III). In Glioblastoma this correlation is just under the level of significance (Fig.1B).

To further characterize the localization of the focally enhanced B7H3-expression, co-stainings with CD31 for endothelial cells, smooth muscle cell actin (SMA) for pericytes or nestin for glioma cells were done (Fig. 1C). These co-localization studies revealed that B7H3 is expressed by endothelial cells and also weakly by SMA-positive cells but in particular by the primary glioma cells surrounding the vessels (Fig. 1CI). On the cellular level, B7H3 protein was expressed in the cytoplasm and on cell membranes.

Moreover, four glioma-initiating cell (GIC) cultures (Suppl. Fig. 1), which were established from human glioblastoma tissue and kept under stem cell conditions, expressed B7H3 mRNA, as did five of five glioma cell lines. To rule out that expression of 4IgB7H3 in vessels of brain tumor tissue (Fig. 1) is due to soluble B7H3 from the glioma cells themselves we performed expression studies of B7H3 in cultivated human pericytes and human cerebral microvascular endothelial cells (hCMEC). The expression detected in hCMECs and pericytes was weaker compared with tumor cells (Fig. 2A). B7H3 protein of the predicted size of ~ 100 kDa was detactable in all tested glioma cultures (Fig. 2A upper panel), but the 45 kDa 2IgB7H3 could not be detected in the glioma samples. Finally, B7H3 was detected on the

surface of glioma cell lines and GIC cultures as assessed by flow cytometry (Fig. 2A). There was no significant difference in B7H3 expression between GIC cultures and cell lines (Fig. 2A).

In an attempt to detect the recently published [24] soluble 16.5 kDa fragment of B7H3 in cell culture supernatants, we used two different antibodies: one directed against a peptide sequence in the first N-terminal immunoglobulin-like extracellular domain, the other one detecting the entire extracellular protein moiety of 2IgB7H3 and in addition due to sequence homology also 4IgB7H3 (Suppl. Fig 3). The existence of a 16.5 kDa fragment could be substantiated neither in supernatant of glioma cell line cultures nor GIC cultures with these commercial antibodies (Fig. 2B).

In order to further analyze the mechanism of soluble 4IgB7H3 secretion, we first examined whether 4IgB7H3 could be detected in the exosomal compartement of LN-229 cells. Indeed, 4IgB7H3 co-localized with the exosomal marker CD9 [36] after exosome preparation but was not detected in the unconcentrated supernatant fraction (Fig. 2C). Comparing 4IgB7H3 originating from cell lysates directly with its secreted form obtained from cell culture supernatants a size difference of about 5-7 kDa was detected in immunoblot analyses (Fig. 2D). In nanoLC electrospray-tandem-massspectrometry analyses this size difference was confirmed, due to a missing peptide sequence of about 7 kDa in the supernatant probe. This part represents the intracellular and transmembrane fragment of 4IgB7H3 (Fig. 2D), which is not present in the concentrated supernatant fraction analysed by two different antibodies. From this we assume that after exosomal release of 4IgB7H3 by glioma cells a 93 kDa fragment is processed and can be detected in concentrated supernatant. 4IgB7H3 appears to be the major isoform of B7H3 expressed in glioblastoma.

**4IgB7H3 is released into the supernatant and inhibits NK-mediated lysis of glioma cells *in vitro* and *in vivo*.**

We next evaluated the functional activity of 4IgB7H3 expressed by glioma cells. 4IgB7H3 was silenced in the glioma cell line LN-229 with a lentiviral system. The initial knockdown has

been about 80% effective, after clonal selection the knock-down reached 93% in clone 19 on the mRNA level. Immunoblot and flow cytometry reveal a clear reduction of 4IgB7H3 protein levels in lysates, supernatant and on the surface of the knockdown cells (Fig. 3A). Of note, the transfectants and control cells do not differ in morphology, generation time or clonogenicity (data not shown). LN-229 sh-4IgB7H3 cells were more susceptible to NK cell-mediated lysis. The clonal knockdown was lysed best with around 60% specific lysis at a target to effector cell ratio of 1 to 30, the less-efficient B7H3-silenced pool transfectants showed an intermediate lysis at 40% while the controls were at 25% (Fig. 3B, left panel). Given that 4IgB7H3 is released into the supernatant, we also analyzed whether soluble glioma cell-derived 4IgB7H3 suppresses NK cell-mediated lysis. Hence, we performed NK lysis assays with LN-229 sh-4IgB7H3 clone 19 cells, which were susceptible to lysis, and supplemented supernatant of LN-229 sh-4IgB7H3 clone 19 or control cells. Compared with the specific NK-mediated lysis of LN-229 sh-4IgB7H3 clone 19 cells of around 60%, the specific lysis of these cells was reduced to 20% by coincubation with concentrated supernatant of control cells. This reduction of specific lysis was weaker after diluting the control supernatant 1:100. The supernatant of LN-229 sh-4IgB7H3 clone 19 cells does not reduce the lysis of LN-229 sh-4IgB7H3 clone 19 cells (Fig. 3B, right panel). We also generated 4IgB7H3 knockdown cells of the GIC culture T269, with a knockdown of 80% on mRNA level and a significant reduction on protein level measured by immunoblot and flow cytometry (Fig. 3C). T269 sh-4IgB7H3 cells, too, have been significantly more susceptible to NK cell-mediated lysis (Fig. 3D). Taken together, these data indicate that 4IgB7H3 and its secreted form suppress NK-cell mediated lysis of glioma cells and GICs *in vitro*.

To further characterize the impact of 4IgB7H3 expression *in vivo,* subcutaneous tumors were generated with LN-229 sh-4IgB7H3 and control cells. Tumor growth was monitored in LN-229 sh-4IgB7H3 and control cells in NK cell-depleted compared with control-IgG-antibody treated mice [37]. Here, a significant difference in tumor growth and tumor weight at the end of the experiment was only detected between LN-229 sh-4IgB7H3 derived tumors in NK cell-depleted *versus* non-depleted animals. In NK cell-retaining animals LN-229 sh-4IgB7H3

derived tumors grew significantly smaller and were lighter at the end of the experiment. In LN-229 sh-control derived tumors NK cell depletion had no significant impact on tumor growth and weight (Fig. 4A-B) demonstrating that silencing of 4IgB7H3 made glioma cells susceptible to NK cell dependant cytotoxicity. Moreover, human glioblastoma samples showed a highly significant inverse correlation between B7H3 expression and invasion of CD8 positive immune cells. Co-staining of B7H3 and CD8 revealed that the influx of CD8 positive cells is significantly higher in B7H3-low expressing tumors compared with B7H3-high expressing tumors (Fig. 4C-D)

**Regulation and cleavage of 4IgB7H3 in glioma cells differ from other tumor entities and immune cells**

To evaluate how 4IgB7H3 expression is regulated and how soluble 4IgB7H3 is cleaved from the cell surface, we assessed the influence of proteinkinase C activation by phorbol 12-myristate 13-acetate (PMA), inhibition of MMP by ilomastat [22], inhibition of TGF-β with LY2157299 or a furin inhibitor and hypoxia on 4IgB7H3 levels. All compounds are sufficiently active in control assays (data not shown). 4IgB7H3 was neither induced by PMA on mRNA level nor on the protein level in cell lysates or with regard to the 93 kDa soluble form in the supernatant of glioma cells (Suppl. Fig.2A). Moreover, cleavage of 4IgB7H3 from the surface of the glioma cell line LN-229 (Suppl. Fig.2B) and GIC cultures T325 (Suppl. Fig.2A,B) was not influenced by inhibition of MMP with ilomastat as shown before for monocytes, DC, activated T-cells and various carcinoma cells. Inhibition of TGF-β, which is known to suppress NK cells and to convey immune escape of gliomas in various manners [38], did not result in down-regulation of 4IgB7H3 nor did hypoxia influence its expression (Suppl. Fig.2A). Further experiments evaluating the regulation of 4IgB7H3 in glioma cells did not show a significant upregulation of 4IgB7H3 on the mRNA level nor in the supernatant of LN-229 cells following irradiation, interferon-γ-, dexamethasone- or $H_2O_2$-treatment (Suppl. Fig 2C).

**4IgB7H3 modulates the invasive phenotype in glioma cells *in vitro* and *in vivo***

Mounting evidence suggests that 4IgB7H3 is involved in tumor cell migration and invasiveness. Therefore, Boyden chamber matrigel and spheroid invasion assays were performed with LN-229 cells as well as with the GIC culture T269. LN-229 sh-4IgB7H3 cells displayed reduced transmigration compared with control cells in these assays (Fig. 5A). Interestingly, the invasive phenotype was partly restored in LN-229 sh-4IgB7H3 cells when invasion assays were conducted with supplementation of concentrated supernatant of LN-229 control cells (Fig. 5B). There was also a reduction in the invasiveness of LN-229 control cells when the cells were incubated with supernatant from LN-229 sh-4IgB7H3 cells instead of supernatant from control cells during the invasion experiments (Fig. 5B), indicating that glioma supernatant may have an anti-invasive property, which can be partly overcome by the pro-invasive effect of soluble 4IgB7H3. To verify this proinvasive effect of 4IgB7H3 in primary glioma cells, primary 4IgB7H3-silenced T269 GICs were further used in a functional invasion assay. This spheroid invasion assay demonstrated a significant reduction of the invasive phenotype in T269 cells after 4IgB7H3 gene silencing (Fig. 5C).

Aiming at confirming the *in vitro* data in an *in vivo* model, T269 sh-4IgB7H3 knock-down or control cells were orthotopically implanted into the brains of CD1 *nu/nu* mice. Ten weeks later, animals were sacrificed and tumor invasion was assessed by staining of the tumor cells with anti-human nestin antibody. Brain sections displayed a highly infiltrative tumor growth pattern with tumor cells reaching brain regions in the ipsi- and contralateral hemisphere far off the implantation site in T269 control xenograft animals (Fig. 6, upper panel). In contrast, clearly defined bulky tumors were found in T269 sh-4IgB7H3 xenografted brains without detectable tumor cells in ipsi- or contralateral brain regions distant from the implantation site (Fig. 6, lower panel).

## Discussion

Glioblastoma is a paradigmatic tumor for tumor-associated immunosuppression. B7H3 is a novel member of the B7-family of costimulatory proteins. As parts of our efforts to characterize and understand the immune phenotype of glioblastoma we here report that B7H3 is expressed in human glioblastoma tissue by both glioblastoma and endothelial cells (Fig. 1 and 2A). Glioma cells, which surround the blood vessels preferentially express B7H3. In addition to that, expression correlates significantly with increasing tumor grade and is associated with poor survival within WHO grade III gliomas.

By mass spectrometry and immunoblot analysis, we identified that 4IgB7H3 but not the smaller isoform 2IgB7H3 was preferentially expressed by different GIC cultures and glioma cell lines what was not determined in immune histochemistry analysis due to the lack of isoform specific antibodies (Suppl. Fig.3). Furthermore, it was demonstrated that 4IgB7H3 is secreted in exosomes into the supernatant of glioma cells and finally processed to a soluble form of about 93 kDa. Interestingly, this soluble 4IgB7H3 is not the 16.5 kDa soluble form of B7H3 postulated in non-malignant and malignant cells before [22]. Although two different antibodies were used, the one detecting whole extracellular protein, the other one the first immunoglobulin-like domain of the extracellular N-Terminus, we could not detect the published fragment of about 16.5 kDa in the supernatant of glioma cells. Here, the soluble fragment was about 7 kDa smaller than 4IgB7H3 originating from cell lysates (Fig. 2). In an attempt to further characterize the regulation and cleavage mechanism of B7H3 in glioblastoma, the cells were incubated with phorbol myristate acetate (PMA), which was published to induce B7H3 on immune and tumor cells [9, 39]. This regimen had no effect on B7H3 expression in glioblastoma cells on mRNA or protein level, neither did the inhibition of MMP, which have been suggested to cleave soluble B7H3 from the surface of tumor cells [22]. We finally evaluated whether blockage of TGF-β activation with a furin inhibitor in the glioblastoma cell line LN-229 influenced 4IgB7H3 expression since TGF-β is known to be responsible for a variety of immunosuppressive and proinvasive effects [5, 6, 8, 20].

However, TGF-β inhibition did neither result in the down-regulation of 4IgB7H3 nor its soluble form (Suppl. Fig.2).

Importantly, 4IgB7H3 was functional in the glioblastoma cell line LN-229 and the GIC culture T269 and suppressed NK cell-mediated tumor lysis *in vitro* (Fig. 2) as well as *in vivo (Fig. 3)*. In attempt to illucidate the immunosuppressive function of B7H3 in human glioblastoma we performed co-localization studies of B7H3 expression and CD8 positive cells. Here, a significant higher influx of CD8 positive cells in B7H3 low expressing tumors was detected compared with B7H3 high expressing tumors. As CD8 is a marker for cytotoxic T-cells which were also published to be suppressed by B7H3 [20] and NK-cells this data provide further evidence for an immunosuppressive function of B7H3. Furthermore, 4IgB7H3 exerted a proinvasive effect in glioblastoma cells *in vitro* (Fig. 5). We could additionally demonstrate the proinvasive effect of 4IgB7H3 in the GIC compartment *in vivo*: the highly invasive phenotype of the GIC culture T269 was significantly reduced by 4IgB7H3 gene silencing (Fig. 6). Interestingly, native glioblastoma-derived soluble 4IgB7H3 suppresses NK lysis and enhances glioblastoma cell invasiveness *in vitro.* Insofar, our data let us to postulate that NK cell suppression and the pro-invasive effect attributed to 4IgB7H3 expression in different tumor entities [39] are in fact exerted by membrane-bound and soluble B7H3, which was until now only evaluated for its diagnostic and prognostic capacity [22, 23, 40]. Finally, as soluble 4IgB7H3 was sufficient to restore the invasiveness of 4IgB7H3-silenced LN-229 cells, the presence of a yet unknown counter-receptor must be postulated on glioblastoma cells, too.

To summarize, our data provide new insights on the role of B7H3 expression in glioblastoma. There is an immunosuppressive function of 4IgB7H3 in glioblastoma similar to other tumor entities. This is also true for a pro-invasive phenotype. These effects can be exerted by secreted soluble 4IgB7H3 on its own leading to the assumption that the yet unidentified counter-receptor is expressed on immune and glioblastoma cells. Glioblastoma unlike non-malignant cells do not generate and release the 16.5 kDa B7H3 fragment into the supernatant analyzed by commercially available antibodies. Our data support a fragment of about 93 kDa to exert that effect rather than a small 16.5 kDa fragment.

These data provide a therapeutic rationale to ameliorate treatment of glioblastoma by blockage of 4IgB7H3. First attempts to use 4IgB7H3 as a therapeutic target have been made recently with an antibody against 4IgB7H3 used to track neuroblastoma cells without intending to block 4IgB7H3 function itself [41], and a pseudomonas immunotoxin-coupled anti-B7H3 antibody to track glioblastoma xenograft tumors [42]. Further experiments are needed to evaluate 4IgB7H3 as a target in the treatment of 4IgB7H3-expressing tumors.

## Figure Legends

**Figure 1.** Expression of B7H3 in human glioma tissue and correlation with the grade of malignancy

**(A)** Gliomas of different WHO grade were analyzed for B7H3 expression by immunohistochemistry. Representative figures and statistical analysis are presented. B7H3 expression is enhanced in proximity to the blood vessels (specimen 1, arrows). Specimen 2 demonstrates upregulated B7H3 in the tumor compared with the surrounding brain tissue (arrow heads). **(B)** Kaplan-Meier survival plot according to Rembrandt queries shows survival of glioma patients with intermediate and high B7H3 expression levels. **(C)** Immunofluorescence microscopy **(I-IV)** was applied to detect B7H3 in three different glioblastoma specimens (T1462, T1297, T1563). Vessels are visualized by CD31 staining, pericytes are stained with $\alpha$-smooth muscle cell actin ($\alpha$-SMA), glioma cells are marked by nestin staining, nuclei are counterstained with DAPI. **($I_{1-2}$)** Glioblastoma cells (white arrowheads) surrounding blood (grey arrowheads) vessels exhibit a higher expression of B7H3.

**Figure 2.** Expression and secretion of 4IgB7H3 by glioma cells, pericytes and endothelial cells.

**(A)** Expression of 4IgB7H3 in pericytes and endothelial cells as well as GIC (black bars) and glioma cell lines (white bars) on mRNA or protein levels **(**right, upper panel**)** and on the cell surface of GIC cultures **(**right, lower panel) is presented.

**(B)** 4IgB7H3 in LN-229 glioma cells and GIC culture S24 was detected in lysates and in concentrated supernatant. A ˜93 kDa fragment was substantiated in the supernatant but no 16.5 kDa fragment. $\alpha$-tubulin was chosen as loading control for cell lysates and Ponceau staining for supernatant. **(C)** Exo preparation demonstrates that 4IgB7H3 is released within the exosomal compartment from the glioma cell line LN-229. CD9 staining was used as a exosomal marker. Unconcentrated supernatants (SN) are negative while lysates (Lys) are positive for for 4IgB7H3 and CD9.

**(D)** Protein size analyzes of 4IgB7H3 in LN-229 whole cell lysates (Lys) and concentrated supernatant (SN) by immunoblot show size differences of whole and soluble 4IgB7H3. Positions of identified peptides (bold letters) in human 4IgB7H3 amino acid sequence deriving from lysates and supernatant analyzed by nanoLC-ESI-MSMS (right panel) as well as illustrative sketch visualizing hypothetical position of soluble 4IgB7H3 processing (interrupted line).

**Figure 3.** Increased susceptibility of LN-229 4IgB7H3 sh-cells to NK cell-mediated lysis.

**(A)** Polyclonal knock-down and clonal selection (clone 19) of 4IgB7H3 in LN-229 cells were performed. Knock-down efficiency on mRNA level (left panel), protein level (middle panel) and on the cell surface evaluated by flow cytometry are illustrated (right panel).

**(B)** LN-229 sh-4IgB7H3 (polyclonal or clone 19), sh-control cells, or LN-229 sh-4IgB7H3 (left panel) as well as clone 19 cells supplemented with supernatant (SN) derived from clone 19 or control cells (right panel) were incubated with activated NK cells for 4 h at the indicated effector to target cell ratios.

**(C)** Knock-down of 4IgB7H3 in GIC culture T269 was performed and efficiency evaluated on mRNA level by qPCR (left panel), on protein level by immunoblot analysis and by flow cytomety (right panel).

**(D)** Activated NK cells were incubated with T269 sh-4IgB7H3 or sh-control cells and NK cell-mediated lysis [%] has been evaluated. Representative results from three independent NK lysis experiments are depicted.

Data represent mean and standard error of the mean (SEM); n=5; *p<0.05 relative to controls.

**Figure 4.** B7H3 exerts an immunosuppressive function *in vivo*

**(A)** Tumor size of subcutaneously injected LN-229 shB7H3 and control cells were monitored in NK-cell depleted (+Asialo) and control treated (+ Isotype) animals. Only the tumors which developed from LN-229 shB7H3 cells growing in mice with NK cells (dotted line) are significantly smaller.

**(B)** Representative images of explanted tumors and statistical analysis of tumor weight at the end of the experiment.

**(C)** B7H3 high-expressing human glioblastoma tissue (specimen 1) shows a reduced infiltration of CD8 positive immune cells compared with B7H3 low-expressing human glioblastoma tissue (specimen 2).

**(D)** Statistical analysis of B7H3 high- and low-expressing human glioblastoma tissues demonstrates a stronger invasion of CD8 positive cells in B7H3 low-expressing tumors.

**Figure 5.** 4IgB7H3 mediates a proinvasive phenotype in glioma cells *in vitro*.

**(A)** LN-229 sh-4IgB7H3 (polyclonal knockdown and clone 19) and sh-control glioma cells or **(B)** clone 19 and sh-control cells incubated each with concentrated supernatant (SN) of control or clone 19 cells were analyzed for invasiveness in a matrigel invasion chamber assay. Invaded cells were counted in five independent fields. Invasion is expressed as percentage in relation to sh-control cells without supernatant (scale bars: 100 µm; data represent mean and standard error of mean (SEM); n=3, p<0.05). Representative photographs of the Boyden chambers are depicted. **(C)** T269 control or sh-4IgB7H3 cells were analyzed for their invasive properties in a spheroid invasion assay. The area covered

by invaded cells from each spheroid was measured in intervals of 24 h. Data represent mean and SEM (n=3). Representative glioma spheroids are shown (scale bars 100 µM).

**Figure 6.** 4IgB7H3 drives the proinvasive phenotype of glioblastoma *in vivo*.
Immunohistological analysis of **(A)** T269 control and **(B)** T269 sh-4IgB7H3 tumor bearing CD1 *nu/nu* mice. T269 tumor cells were detected by immunoflurescent anti-human nestin staining. Asterisks show areas with a higher magnification.

**Suppl. Figure 1.** GIC cultures used for this work fulfill the criteria of tumor-initiating cells.
Stem cell characteristics of the used GIC cultures are shown exemplary for T269. **(A)** T269 forms spheres when cultured in serum free medium supplemented with the growth factors EGF and bFGF. **(B and C)** T269 is positive for the progenitor marker nestin and can be differentiated by growth factor removal and serum supplementation. In response to differentiation, Tuj1 and GFAP are upregulated as demonstrated with immune fluorescence microscopy and flow cytometry. **(D)** T269 is highly tumorigenic after orthotopic implantation of as few as 50 cells into CD1 *nu/nu* mouse brains and forms a highly invasive tumor as demonstrated by HE staining. **(E)** Shows tumor initiation capacity of GIC cultures T269, T325, T323 and T1 after orthotopic implantation of $10^3$ and 5 x $10^4$ cells in CD1 nu/nu mice.

**Suppl. Figure 2.** Regulation of 4IgB7H3-expression and cleavage of soluble 4IgB7H3.
**(A)** Relative 4IgB7H3 mRNA or protein levels in lysates and supernatant as well as protein surface levels were evaluated in LN-229 after treating the cells with hypoxia, ilomastat, a furin-inhibitor and PMA (grey bars). Control treatments (white bars) show no significant differences.
**(B)** Ilomastat does not alter the content of B7H3 on the surface of GIC culture T325 in flow cytometry.
**(C)** Irradiation with 8 Gy, treatment with $H_2O_2$, dexamethasone and IFN-γ do neither increase 4IgB7H3 expression on mRNA level nor in the supernatant.

**Suppl. Figure 3.**

Anti-human B7-Homolog3 antibody from R&D is directed against Leu29-Pro245 (red color) of 2IgB7H3. The illustration demonstrates sequence homology (red) of this section in 2Ig and 4IgB7H3 explaining detection of both isoforms by the polyclonal antibody ...

**Suppl. Figure 4.**

In order to prove the specificity of the 4IgB7H3 stains for flow cytometry, 4IgB7H3-containing supernatant of LN-229 wild type cells was added to the cells during the staining procedure. This measurement led to a reduction of the fluorescence intensity (grey curve) compared with the untreated probes (black curve) while the isotype control remained unchanged.

**Acknowledgements**

This work was supported within the Brain Tumor Network BTNplus (Subproject 14; FKZ 01GS0883) of the National Genome Research Network (NGFNplus) by the Federal Ministry of Education and Research (BMBF), and the Charitable Hertie Foundation.

We thank Marius Lemberg, Center for Molecular Biology, University of Heidelberg, Germany for advice with the exosome preparation. We also like to thank for the support by the Microscopy Core Facility and the Department of Molecular Genetics (B. Radlwimmer) of the German Cancer Research Center Heidelberg, Germany.

Reference List

[1] Dietrich PY. Antitumor immune response: what are the roles for gliomas?. Rev Neurol. (Paris) 2001;157:1339-48.

[2] Eisele G, Wischhusen J, Mittelbronn M, Meyermann R, Waldhauer I, Steinle A, et al. TGF-beta and metalloproteinases differentially suppress NKG2D ligand surface expression on malignant glioma cells. Brain 2006;129:2416-25.

[3] Friese MA, Wischhusen J, Wick W, Weiler M, Eisele G, Steinle A, et al. RNA interference targeting transforming growth factor-beta enhances NKG2D-mediated antiglioma immune response, inhibits glioma cell migration and invasiveness, and abrogates tumorigenicity in vivo. Cancer Res. 2004;64:7596-603.

[4] Heimberger AB, Kong LY, Abou-Ghazal M, Reina-Ortiz C, Yang DS, Wei J, et al. The role of tregs in human glioma patients and their inhibition with a novel STAT-3 inhibitor. Clin Neurosurg. 2009;56:98-106.

[5] Roth P, Aulwurm S, Gekel I, Beier D, Sperry RG, Mittelbronn M, et al. Regeneration and tolerance factor: a novel mediator of glioblastoma-associated immunosuppression. Cancer Res. 2006;66:3852-8.

[6] Roth P, Mittelbronn M, Wick W, Meyermann R, Tatagiba M, Weller M. Malignant glioma cells counteract antitumor immune responses through expression of lectin-like transcript-1. Cancer Res. 2007;67:3540-4.

[7] Sampson JH, Archer GE, Mitchell DA, Heimberger AB, Bigner DD. Tumor-specific immunotherapy targeting the EGFRvIII mutation in patients with malignant glioma. Semin Immunol. 2008;20:267-75.

[8] Weller M, Fontana A. The failure of current immunotherapy for malignant glioma. Tumor-derived TGF-beta, T-cell apoptosis, and the immune privilege of the brain. Brain Res Brain Res Rev. 1995;21:128-51.

[9] Chapoval AI, Ni J, Lau JS, Wilcox RA, Flies DB, Liu D, et al. B7-H3: a costimulatory molecule for T cell activation and IFN-gamma production. Nat Immunol. 2001;2:269-74.

[10] Steinberger P, Majdic O, Derdak SV, Pfistershammer K, Kirchberger S, Klauser C, et al. Molecular characterization of human 4Ig-B7-H3, a member of the B7 family with four Ig-like domains. J Immunol. 2004;172:2352-9.

[11] Zhou YH, Chen YJ, Ma ZY, Xu L, Wang Q, Zhang GB, et al. 4IgB7-H3 is the major isoform expressed on immunocytes as well as malignant cells. Tissue Antigens 2007;70:96-104.

[12] Castriconi R, Dondero A, Augugliaro R, Cantoni C, Carnemolla B, Sementa AR, et al. Identification of 4Ig-B7-H3 as a neuroblastoma-associated molecule that exerts a protective role from an NK cell-mediated lysis. Proc Natl Acad Sci U S A 2004;101:12640-5.

[13] Crispen PL, Sheinin Y, Roth TJ, Lohse CM, Kuntz SM, Frigola X, et al. Tumor cell and tumor vasculature expression of B7-H3 predict survival in clear cell renal cell carcinoma. Clin Cancer Res. 2008;14:5150-7.

[14] Roth TJ, Sheinin Y, Lohse CM, Kuntz SM, Frigola X, Inman BA, et al. B7-H3 ligand expression by prostate cancer: a novel marker of prognosis and potential target for therapy. Cancer Res. 2007;67:7893-900.

[15] Sun Y, Wang Y, Zhao J, Gu M, Giscombe R, Lefvert AK, et al. B7-H3 and B7-H4 expression in non-small-cell lung cancer. Lung Cancer 2006;53:143-51.

[16] Yamato I, Sho M, Nomi T, Akahori T, Shimada K, Hotta K, et al. Clinical importance of B7-H3 expression in human pancreatic cancer. Br J Cancer 2009;101:1709-16.

[17] Zang X, Thompson RH, Al-Ahmadie HA, Serio AM, Reuter VE, Eastham JA, et al. B7-H3 and B7x are highly expressed in human prostate cancer and associated with disease spread and poor outcome. Proc Natl Acad Sci U S A 2007;104:19458-63.

[18] Seaman S, Stevens J, Yang MY, Logsdon D, Graff-Cherry C, St CB. Genes that distinguish physiological and pathological angiogenesis. Cancer Cell 2007;11:539-54.

[19] Hashiguchi M, Kobori H, Ritprajak P, Kamimura Y, Kozono H, Azuma M. Triggering receptor expressed on myeloid cell-like transcript 2 (TLT-2) is a counter-receptor for B7-H3 and enhances T cell responses. Proc Natl Acad Sci U S A 2008;105:10495-500.

[20] Leitner J, Klauser C, Pickl WF, Stöckl J, Majdic O, Bardet AF, et al. B7-H3 is a potent inhibitor of human T-cell activation: No evidence for B7-H3 and TREML2 interaction. Eur J Immunol. 2009;39:1754-64.

[21] Sun J, Chen LJ, Zhang GB, Jiang JT, Zhu M, Tan Y, et al. Clinical significance and regulation of the costimulatory molecule B7-H3 in human colorectal carcinoma. Cancer Immunol Immunother. 2010;59:1163-71.

[22] Zhang G, Hou J, Shi J, Yu G, Lu B, Zhang X. Soluble CD276 (B7-H3) is released from monocytes, dendritic cells and activated T cells and is detectable in normal human serum. Immunology 2008;123:538-46.

[23] Zhang G, Xu Y, Lu X, Huang H, Zhou Y, Lu B, et al. Diagnosis value of serum B7-H3 expression in non-small cell lung cancer. Lung Cancer 2009;66:245-9.

[24] Zhang G, Hou J, Shi J, Yu G, Lu B, Zhang X. Soluble CD276 (B7-H3) is released from monocytes, dendritic cells and activated T cells and is detectable in normal human serum. Immunology 2008;123:538-46.

[25] Hermisson M, Klumpp A, Wick W, Wischhusen J, Nagel G, Roos W, et al. O6-methylguanine DNA methyltransferase and p53 status predict temozolomide sensitivity in human malignant glioma cells. J Neurochem 2006;96:766-76.

[26] Svendsen CN, ter Borg MG, Armstrong RJ, Rosser AE, Chandran S, Ostenfeld T, et al. A new method for the rapid and long term growth of human neural precursor cells. J Neurosci Methods 1998;85:141-52.

[27] Rieger J, Lemke D, Maurer G, Weiler M, Frank B, Tabatabai G, et al. Enzastaurin-induced apoptosis in glioma cells is caspase-dependent and inhibited by BCL-XL. J Neurochem. 2008;106:2436-48.

[28] Burghardt I, Tritschler F, Opitz CA, Frank B, Weller M, Wick W. Pirfenidone inhibits TGF-beta expression in malignant glioma cells. Biochem Biophys Res Commun. 2007;354:542-7.

[29] Weiler M, Bähr O, Hohlweg U, Naumann U, Rieger J, Huang H, et al. BCL-xL: time-dependent dissociation between modulation of apoptosis and invasiveness in human malignant glioma cells. Cell Death Differ. 2006;13:1156-69.

[30] Jang BC, Park YK, Choi IH, Kim SP, Hwang JB, Baek WK, et al. 12-O-tetradecanoyl phorbol 13-acetate induces the expression of B7-DC, -H1, -H2, and -H3 in K562 cells. Int J Oncol. 2007;31:1439-47.

[31] Leitlein J, Aulwurm S, Waltereit R, Naumann U, Wagenknecht B, Garten W, et al. Processing of immunosuppressive pro-TGF-beta 1,2 by human glioblastoma cells involves cytoplasmic and secreted furin-like proteases. J Immunol. 2001;166:7238-43.

[32] Opitz CA, Litzenburger UM, Lutz C, Lanz TV, Tritschler I, Köppel A, et al. Toll-like receptor engagement enhances the immunosuppressive properties of human bone marrow-derived mesenchymal stem cells by inducing indoleamine-2,3-dioxygenase-1 via interferon-beta and protein kinase R. Stem Cells 2009;27:909-19.

[33] Carraro G, Albertin G, Forneris M, Nussdorfer GG. Similar sequence-free amplification of human glyceraldehyde-3-phosphate dehydrogenase for real time RT-PCR applications. Mol Cell Probes 2005;19:181-6.

[34] Friese MA, Wischhusen J, Wick W, Weiler M, Eisele G, Steinle A, et al. RNA interference targeting transforming growth factor-beta enhances NKG2D-mediated antiglioma immune response, inhibits glioma cell migration and invasiveness, and abrogates tumorigenicity in vivo. Cancer Res. 2004;64:7596-603.

[35] Wick W, Grimmel C, Wild-Bode C, Platten M, Arpin M, Weller M. Ezrin-dependent promotion of glioma cell clonogenicity, motility, and invasion mediated by BCL-2 and transforming growth factor-beta2. J Neurosci. 2001;21:3360-8.

[36] Opitz CA, Litzenburger UM, Sahm F, Ott M, Tritschler I, Trump S, et al. An endogenous ligand of the human aryl hydrocarbon receptor promotes tumor formation. Nature (in press) 2011.

[37] Guescini M, Genedani S, Stocchi V, Agnati LF. Astrocytes and Glioblastoma cells release exosomes carrying mtDNA. J Neural Transm. 2010;117:1-4.

[38] Wick W, Wild-Bode C, Frank B, Weller M. BCL-2-induced glioma cell invasiveness depends on furin-like proteases. J Neurochem. 2004;91:1275-83.

[39] Chen YW, Tekle C, Fodstad O. The immunoregulatory protein human B7H3 is a tumor-associated antigen that regulates tumor cell migration and invasion. Curr Cancer Drug Targets 2008;8:404-13.

[40] Chen X, Zhang G, Li Y, Feng X, Wan F, Zhang L, et al. Circulating B7-H3(CD276) elevations in cerebrospinal fluid and plasma of children with bacterial meningitis. J Mol Neurosci. 2009;37:86-94.

[41] Kramer K, Kushner BH, Modak S, Pandit-Taskar N, Smith-Jones P, Zanzonico P, et al. Compartmental intrathecal radioimmunotherapy: results for treatment for metastatic CNS neuroblastoma. J Neurooncol. 2009.

[42] Luther N, Cheung NK, Souliopoulos EP, Karampelas I, Bassiri D, Edgar MA, et al. Interstitial infusion of glioma-targeted recombinant immunotoxin 8H9scFv-PE38. Mol Cancer Ther. 2010;9:1039-46.

Fig.1

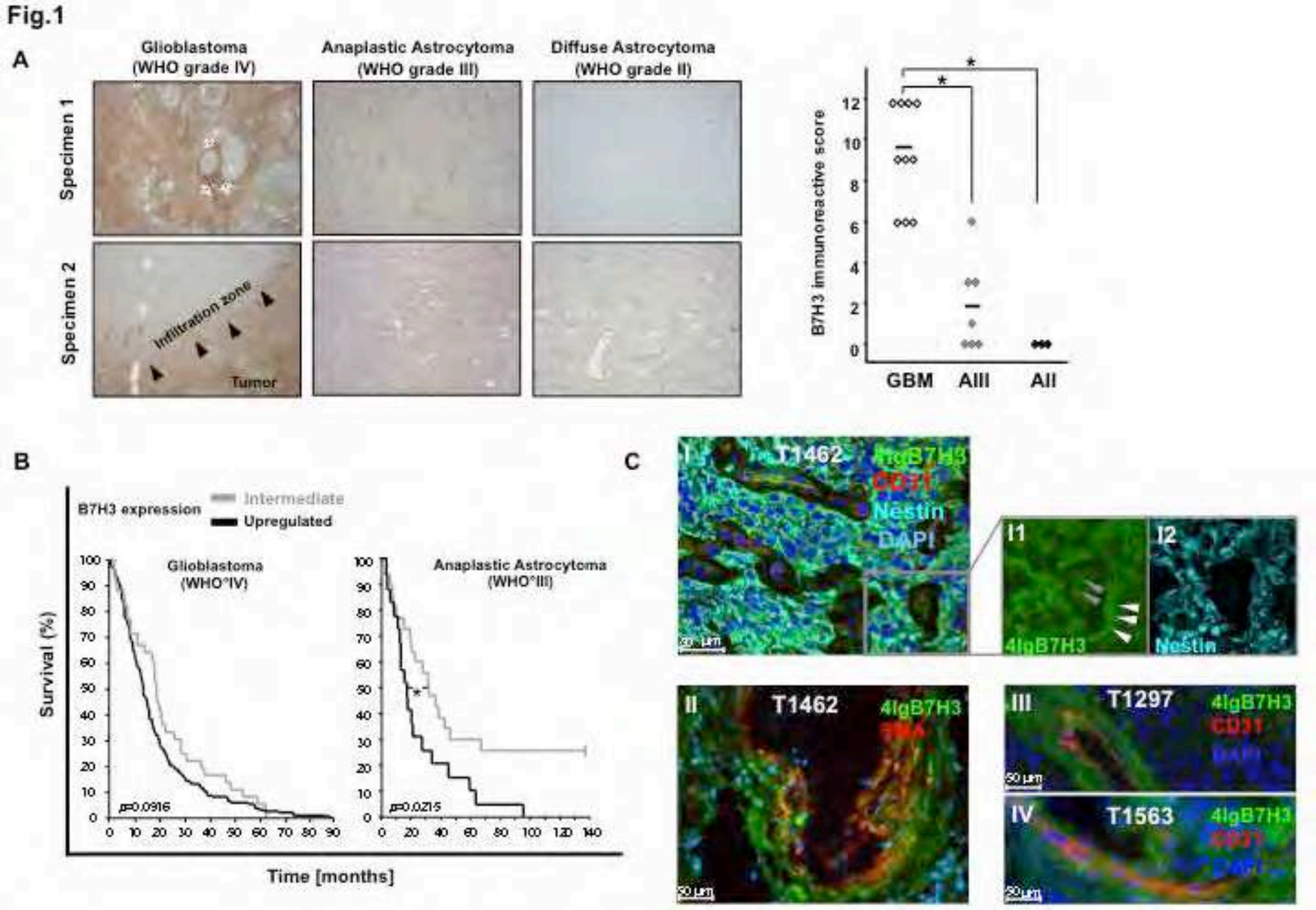
A
Glioblastoma (WHO grade IV)
Anaplastic Astrocytoma (WHO grade III)
Diffuse Astrocytoma (WHO grade II)
Specimen 1
Specimen 2
Infiltration zone
Tumor
B7H3 immunoreactive score
GBM
AIII
AII
B
B7H3 expression
Intermediate
Upregulated
Glioblastoma (WHO°IV)
Anaplastic Astrocytoma (WHO°III)
Survival (%)
Time [months]
p=0.0916
p=0.0215
C
I
T1462
4IgB7H3
CD31
Nestin
DAPI
I1
I2
II
T1462
III
T1297
IV
T1563
50 µm

Fig.2

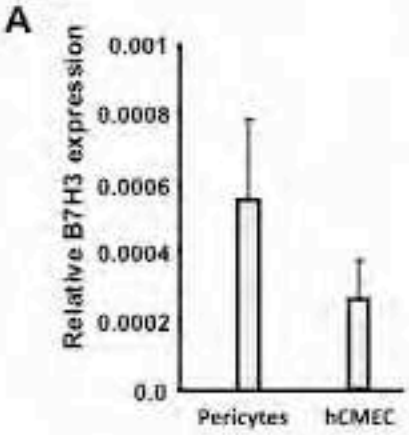
A
Relative B7H3 expression
0.001
0.0008
0.0006
0.0004
0.0002
0.0
Pericytes
hCMEC

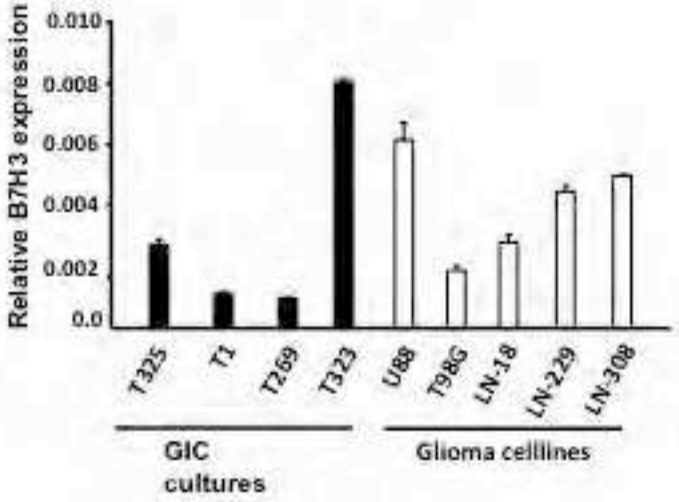
Relative B7H3 expression
0.010
0.008
0.006
0.004
0.002
0.0
T325
T1
T269
T323
U88
T98G
LN-18
LN-229
LN-308
GIC cultures
Glioma cellines

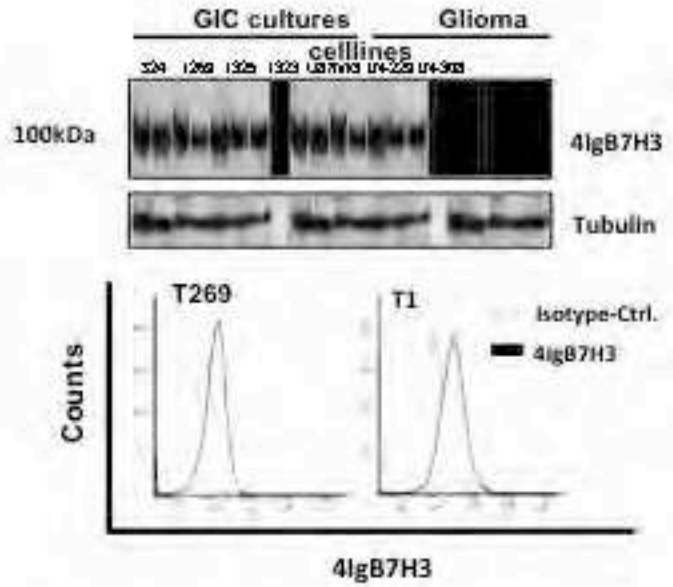
GIC cultures
Glioma
cellines
100kDa
4IgB7H3
Tubulin
T269
T1
Isotype-Ctrl.
4IgB7H3
Counts
4IgB7H3

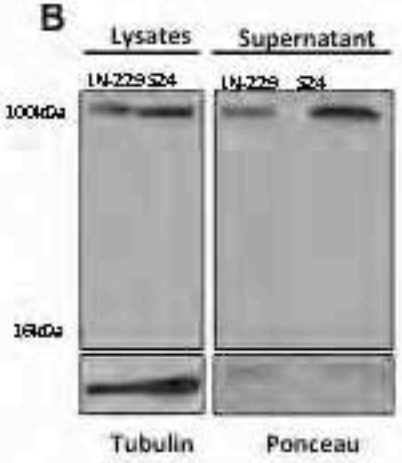
B
Lysates
Supernatant
LN-229
S24
LN-229
S24
100kDa
Tubulin
Ponceau

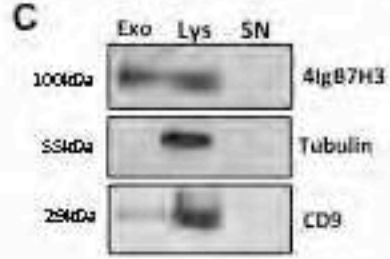
C
Exo
Lys
SN
100kDa
4IgB7H3
55kDa
Tubulin
25kDa
CD9


D
Lys
SN
4IgB7H3
Tubulin
s4IgB7H3
extra
TM
CT
intra
Lysate
Extracellular
Intracellular
Supernatant
Extracellular
Intracellular

Fig. 3

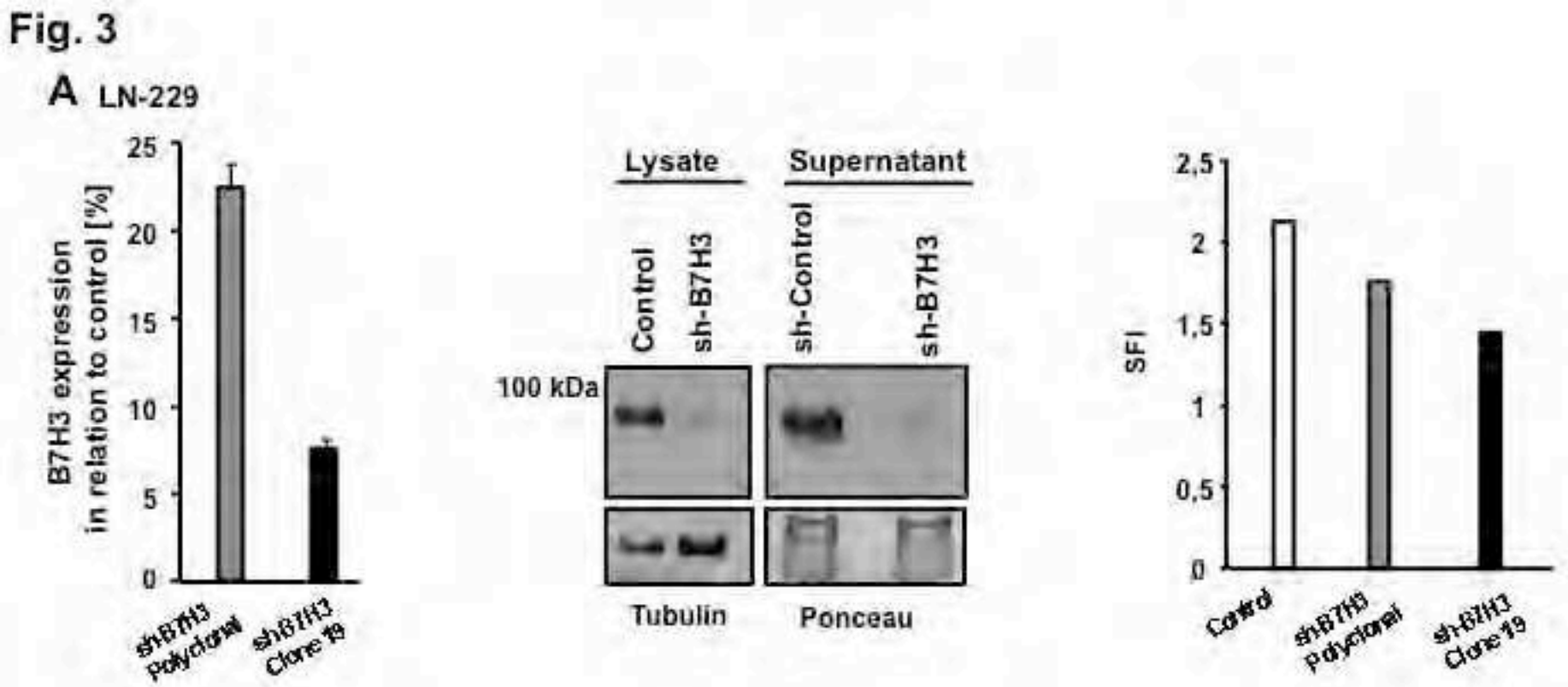
A
LN-229
B7H3 expression in relation to control [%]
25
20
15
10
5
0
sh-B7H3 Polyclonal
sh-B7H3 Clone 19
Lysate
Supernatant
Control
sh-B7H3
sh-Control
sh-B7H3
100 kDa
Tubulin
Ponceau
SFI
2,5
2
1,5
1
0,5
0
Control
sh-B7H3 Polyclonal
sh-B7H3 Clone 19

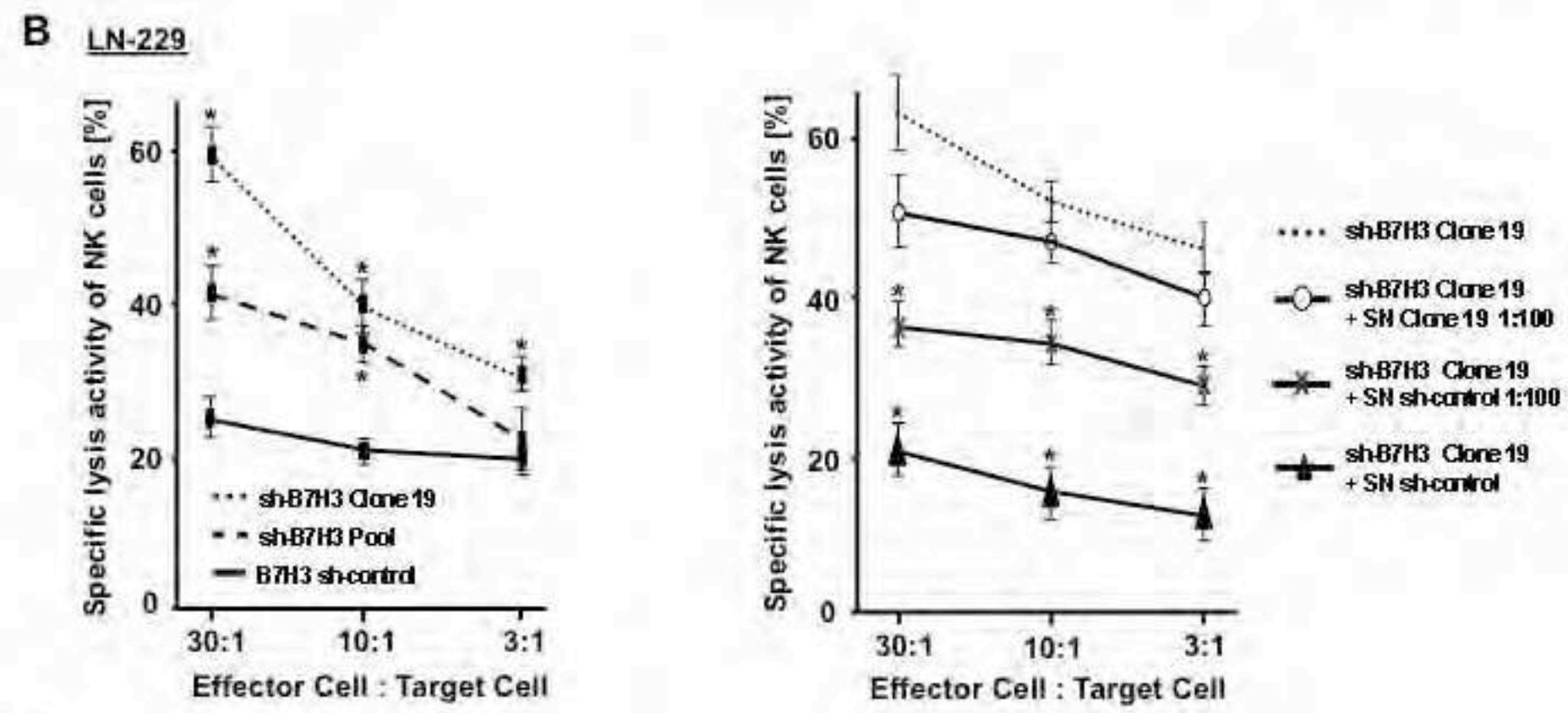
B
LN-229
Specific lysis activity of NK cells [%]
60
40
20
0
sh-B7H3 Clone 19
sh-B7H3 Pool
B7H3 sh-control
30:1
10:1
3:1
Effector Cell : Target Cell
sh-B7H3 Clone 19
sh-B7H3 Clone 19 + SN Clone 19 1:100
sh-B7H3 Clone 19 + SN sh-control 1:100
sh-B7H3 Clone 19 + SN sh-control

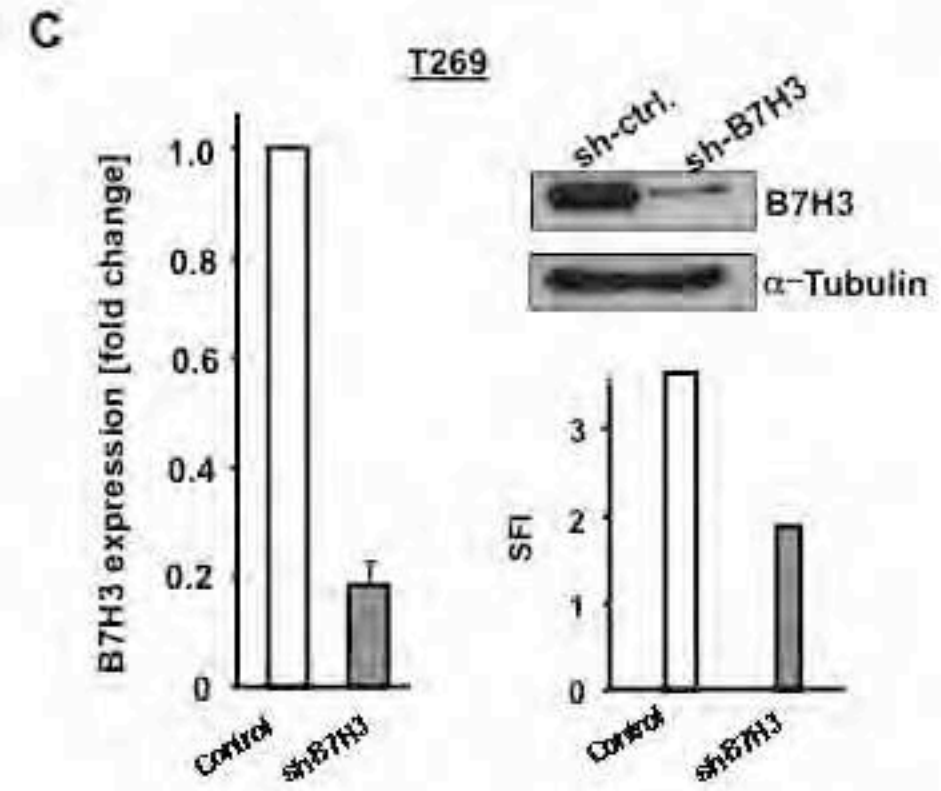
C
T269
B7H3 expression [fold change]
1.0
0.8
0.6
0.4
0.2
0
Control
sh-B7H3
sh-ctrl.
sh-B7H3
B7H3
α-Tubulin
SFI
3
2
1
0
Control
sh-B7H3

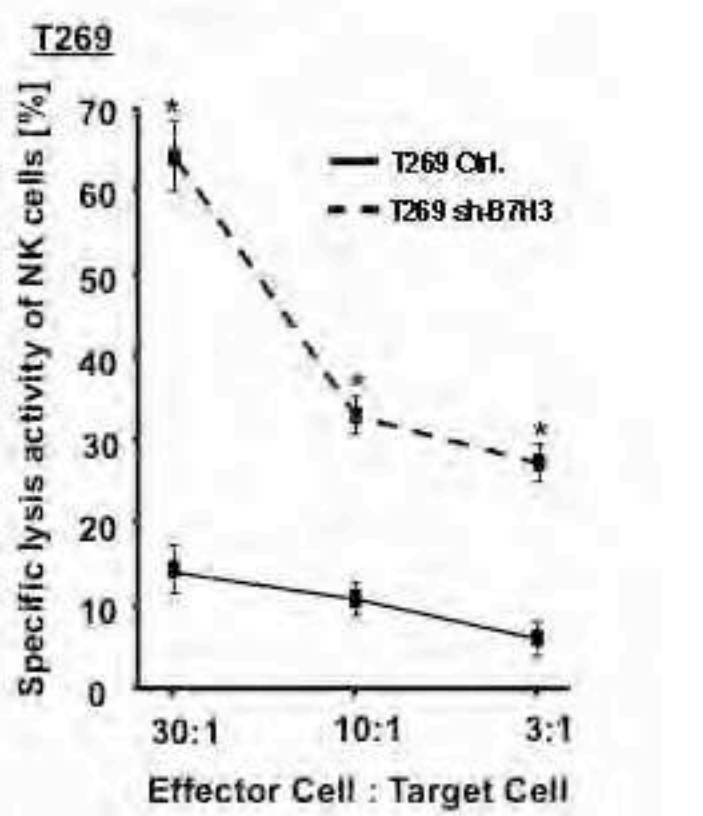
D
T269
Specific lysis activity of NK cells [%]
70
60
50
40
30
20
10
0
T269 Ctrl.
T269 sh-B7H3
30:1
10:1
3:1
Effector Cell : Target Cell

Fig.4

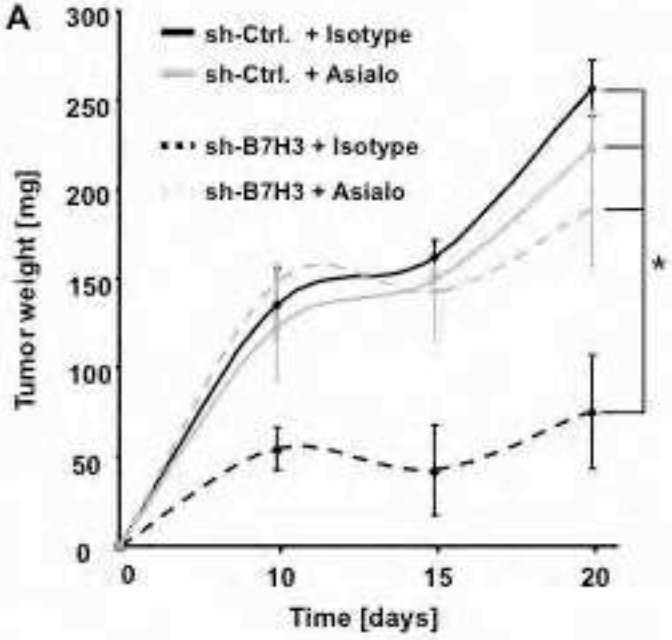
A
sh-Ctrl. + Isotype
sh-Ctrl. + Asialo
sh-B7H3 + Isotype
sh-B7H3 + Asialo
Tumor weight [mg]
Time [days]
0
50
100
150
200
250
300
0
10
15
20
*

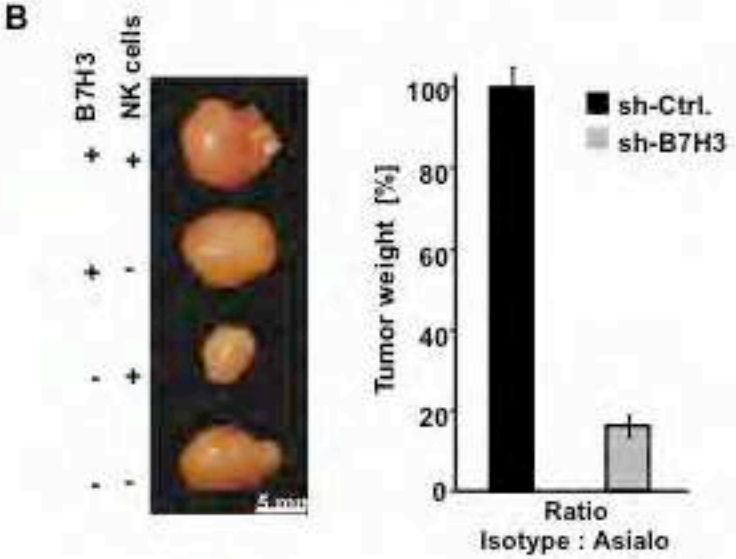
B
B7H3
NK cells
+ +
+ -
- +
- -
sh-Ctrl.
sh-B7H3
Tumor weight [%]
0
20
40
60
80
100
Ratio
Isotype : Asialo

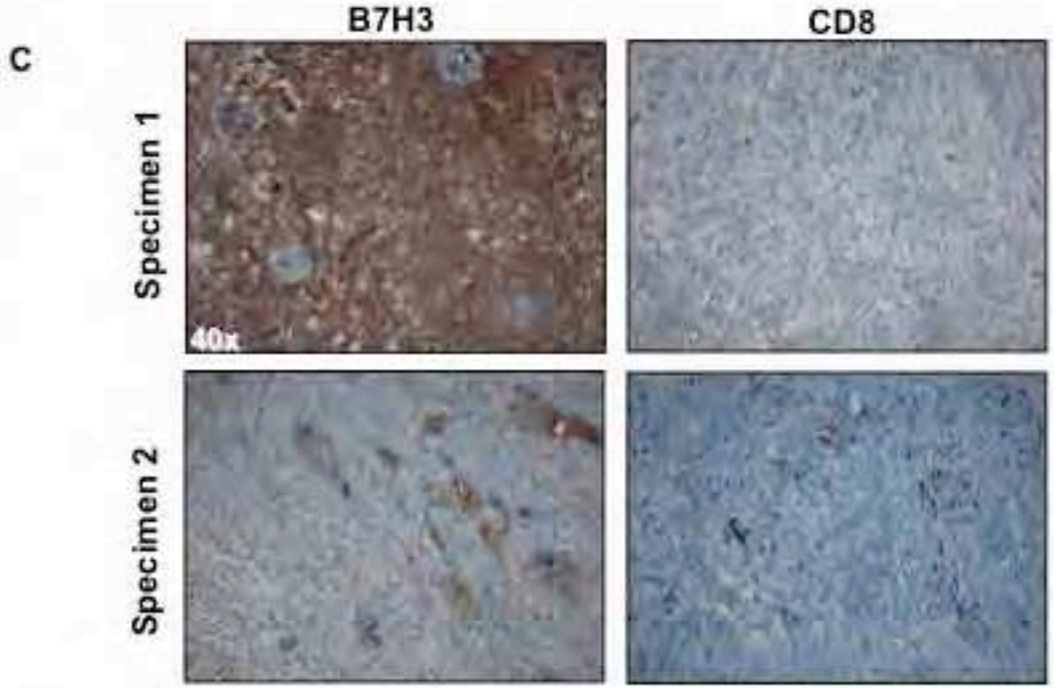
C
B7H3
CD8
Specimen 1
Specimen 2
40x

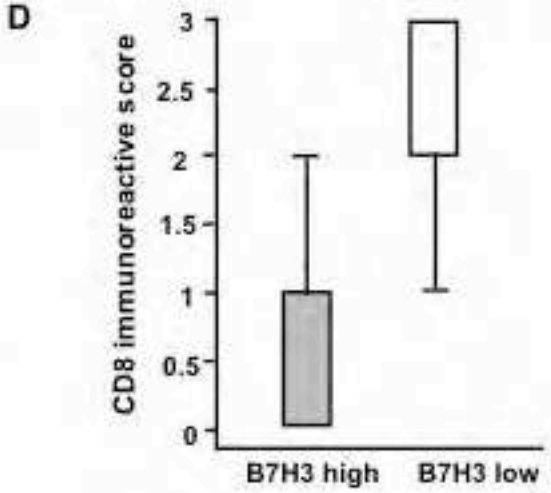
D
CD8 immunoreactive score
0
0.5
1
1.5
2
2.5
3
B7H3 high
B7H3 low

Fig.5

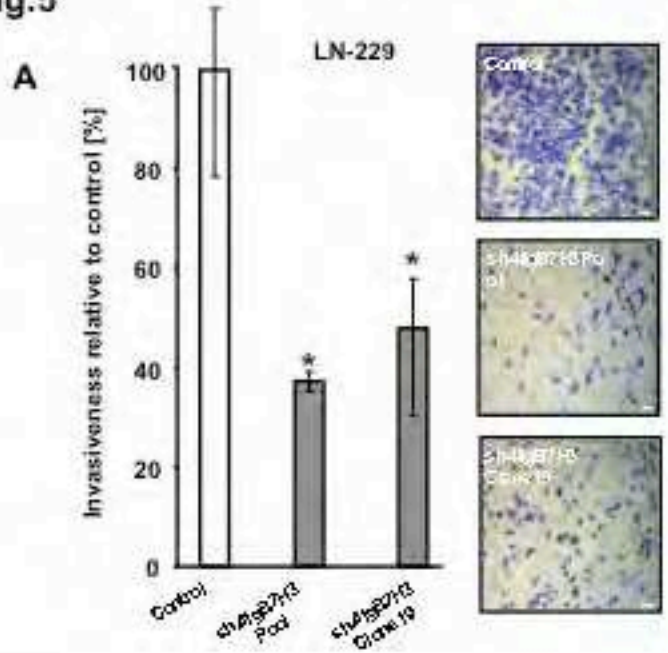
A
LN-229
Invasiveness relative to control [%]
100
80
60
40
20
0
Control
sh-4IgB7H3 Pool
sh-4IgB7H3 Clone 19
Control
sh-4IgB7H3 Pool
sh-4IgB7H3 Clone 19

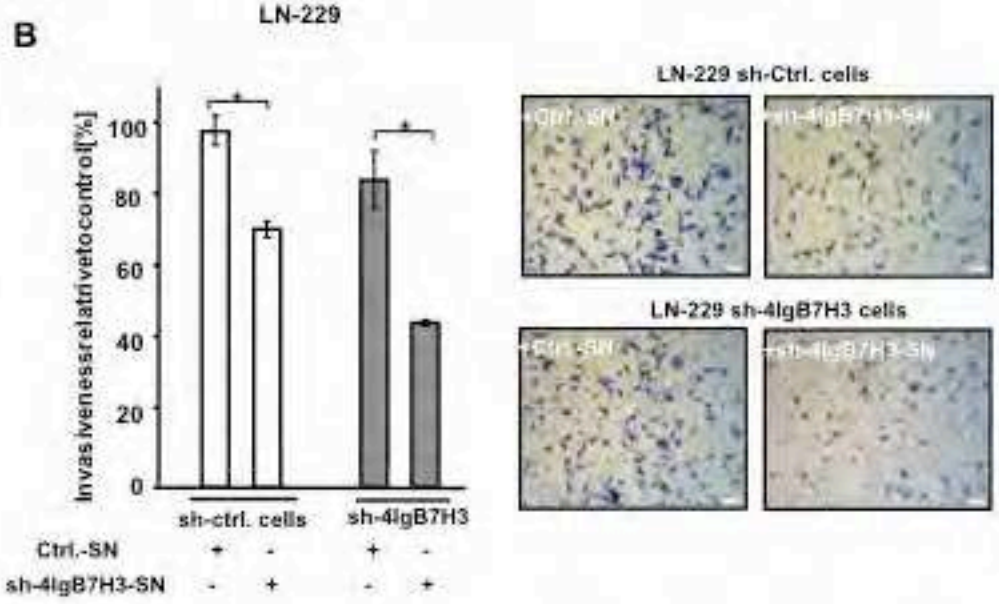
B
LN-229
Invasiveness relative to control [%]
100
80
60
40
20
0
sh-ctrl. cells
sh-4IgB7H3
Ctrl.-SN + - + -
sh-4IgB7H3-SN - + - +
LN-229 sh-Ctrl. cells
LN-229 sh-4IgB7H3 cells

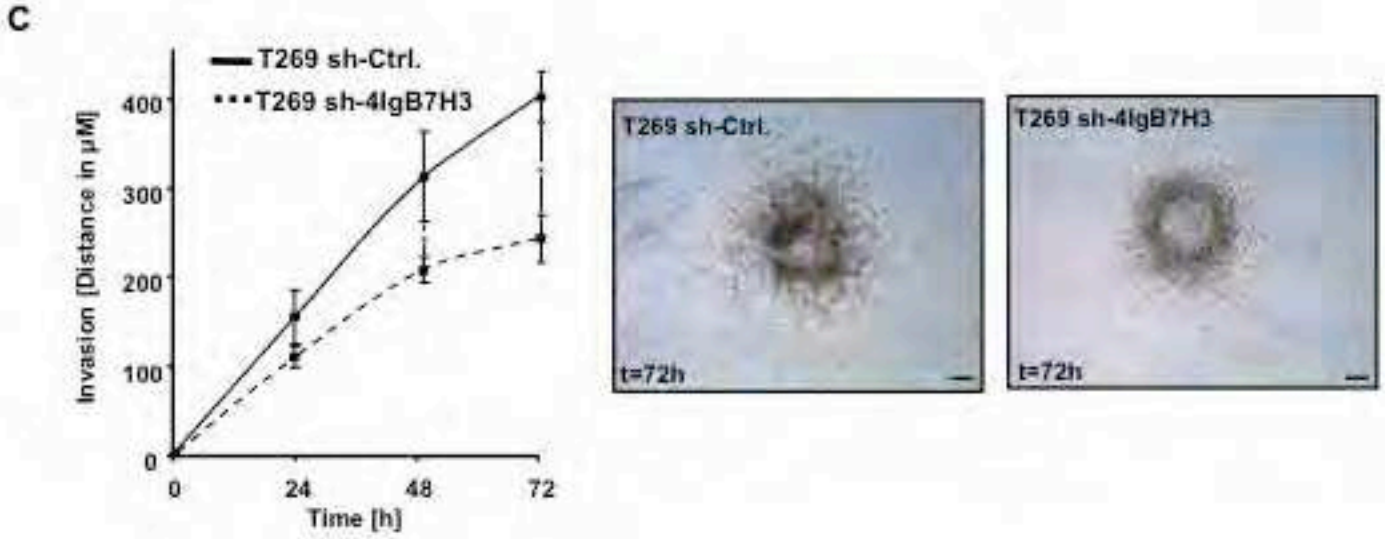
C
T269 sh-Ctrl.
T269 sh-4IgB7H3
Invasion [Distance in µM]
400
300
200
100
0
0
24
48
72
Time [h]
T269 sh-Ctrl.
t=72h
T269 sh-4IgB7H3
t=72h

Fig.6

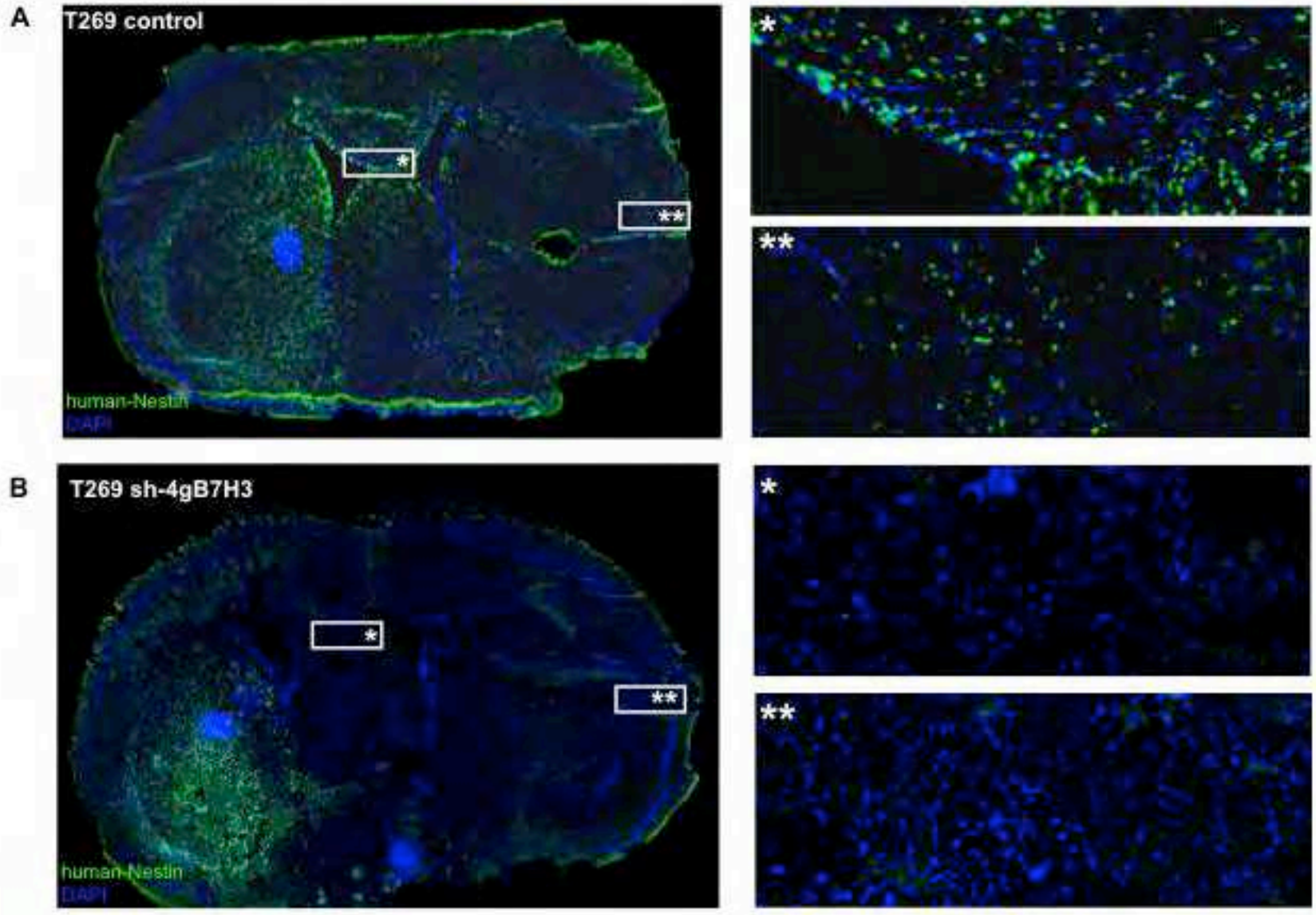
A
T269 control
*
**
human-Nestin
DAPI
*
**
B
T269 sh-4gB7H3
*
**
human-Nestin
DAPI
*
**